International Journal of Engineering Research and Science & Technology

www.ijerst.org

ISSN : 2319-5991

Vol. 22 No. 1(s) (2026)



ijerst.editor@gmail.com

editor@ijerst.com

www.ijerst.com
© 2026 IJERST. All Rights Reserved
Peer Reviewed, Referred & Indexed Journal

Research Paper

Investigation of Structural and Optical Property of Ti Doped Tungsten Trioxide Nano Composites Water Remedial

Aniket Sawant. Tikkal Pallavi, Dnyaneshwar Kolate, Pravin Ghare

Post Graduate Department of Analytical Chemistry, Jijamata College of Science and Arts, Bhende Bk, Tal: Newasa, Dist: Ahilyanagar, Maharashtra, India

Email: ghare pravin93@gmail.com

Abstract

In this paper we have discus tungsten Oxide (WO_3) and metal modified WO_3 composites by using TiO_2 were synthesized using Solgel methods. The changes in particle size due to that surface properties change nanoparticles very popular in the field of nano science. The XRD studies confirmed the formation of orthorhombic WO_3 while FT-IR, verified the presence of Ti-O and W-O bonding environments and enhanced oxygen vacancies. Among the prepared samples, the 2% Ti-doped WO3 photocatalyst (1TW) exhibited superior visible-light activity, achieving 91.84% degradation of 10 ppm methylene blue (MB) within 180 min. using 20 mg catalyst. These findings demonstrate that Ti incorporation is an effective and powerful strategy for tailoring electronic structure significantly improving the photocatalytic efficiency of WO3-based materials for wastewater treatment.

Keywords: Ti-Doped WO_3; Wastewater treatment; Methylene blue; Nanocomposites; Sol-gel method; Photo-degradation

1. Introduction

The term "nano" has gained enormous attention and importance over the past few decades. Nanotechnology is concerned with creating and using particles called nanoparticles (NPs) that range in size from 0.1 nm to 100 nm. A lot of attention has been given to the skillful synthesis of nanohybrids made of noble metals (Au, Ag, Pt, and Pd, as well as Au, Ag alloy) and metal oxides (ZnO, TiO_2, Cu_2O, MnO_2, Fe_2O_3, and CeO_2) for use in various field[1]. It is fastest growing research area because of nearly equal to 90% of chemical process and 80% chemical productions catalyst plays an important role for the satisfy demand for high perform[2]. In recent day the application of NPs in various field such as photocatalyst[3], waste water treatment[4], solar energy[5], Biofuels[6], Semiconductors[7], Agriculture[8], Cosmetics, sunscreen[9], Cancer Treatment, drug delivery[10], gas sensing

Semiconductors[11]. However, among them Tungsten oxides (WO_x) are unique materials[12] due to its numerous uses in the biological, optical, and electronics industries, tungsten oxide nanoparticles have garnered the most interest than any metal oxide nanoparticles[13]. Tungsten oxide WO_3 is a wide band gap (3–3.2) eV. For increasing titanium concentrations, optical tests showed a bandgap renormalization in tungsten oxide films. The films bandgap values drop from 3.17 eV for pure WO_3 to 2.7 eV for 10 weight percent TiO_2 modified WO3 films[14]Due to WO3's band gap being less than 3.0 eV, the system functions when exposed to visible light at 450 nm[15]. The most researched semiconductor photocatalyst is TiO_2[16][18], has applications in transparent protective coatings, electroluminescent devices, dynamic random access memory, and materials with optical band gap energies similar to stoichiometric WO_3[14].

This review will provide a platform for understanding the different synthesis routes and the mechanical study of the applications of tungsten oxide and metal/nonmetal mixed-tungsten oxide WOxNPs to design effective nanocomposites with improved physico-chemical properties for their future applications.

2. Synthesis of pure WO_3

The Tungsten oxide (WO3) nanoparticle were prepaid by taking 3.334 g Sodium tungstate dihydrate (Na2WO4.2H2O) and dissolve it in 30 ml DDW. Sonicated this solution for 5 min., and then added CTAB (0.5 g) to make a clear gel solution with constant magnetic stirring temperature at 70 ℃. The yellow coloured sol dispersion was get form after drop-wise addition 2N HNO3 (20 ml). The slurry was then heated at 70 ℃ for 3 hours to obtain a yellow solid material which was filter, wash with distilled water three times. The final dry mass was calcined at 500 ℃ for 2 hour to obtain pure WO3 (PW) nanocomposite material.by using same procedure synthesize 1% TW. In which titanium isopropanol use as Ti precursor.

3. Characterization Techniques:

By using sophisticated analytical techniques, the synthesized materials were characterized to find out the some important information Fourier Transform Infra-red Spectroscopy (FT-IR) of prepared nanocomposite was analyzed by using PerkinElmer (Spectrum 2) using a Diamond ATR in the region between 3500 to 450 cm-1. The Ultra-violet Visible Diffused reflectance spectra (UV-DRS) of composite were measured by using Lab India UV-Vis spectrophotometer (UV 3092) between the regions of 200-800 nm. Powder X-Ray Diffraction (XRD) analysis of the prepared nanocomposites was recorded on a powder X-ray diffractometer (Rigacu MiniFlex 600) using Cu Kα radiation source with $\lambda = 0.154$ nm. The scanned angle with range of 2θ (°) = 10 to 80.

4. Results and Discussion:

X-ray Diffraction Spectroscopy (XRD) analysis:

The XRD study of all synthesized material was successfully performed and analysis is shown in Figure.1 XRD analysis of pure WO_3 shows high intense peak observed at 2θ (°) values of 23.09, 23.54, 50.48, 55.85 which is corresponding to (002), (020), (200), (241). All planes of the WO_3 perfectly match with orthorhombic crystal structure with JCPDS card No. 71-0131.

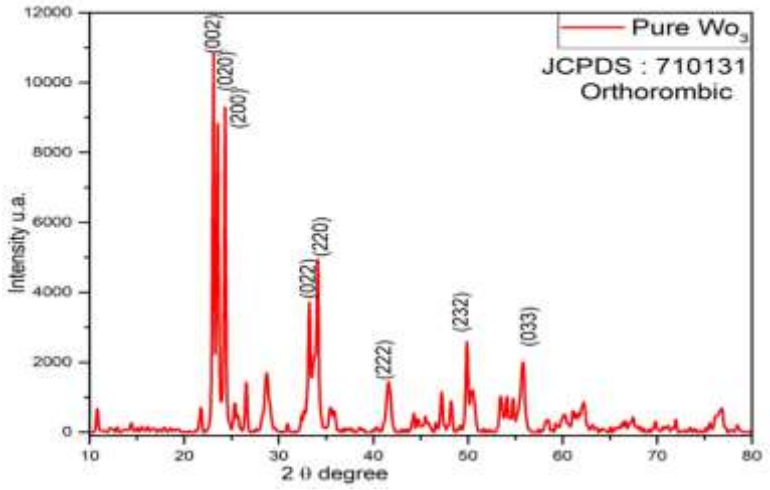


Figure.1 XRD of Pure WO_3

FT-IR Analysis:

The synthesised materials' functional groups and alterations in chemical composition were investigated using FT-IR analysis and shown in Figure.2 The prominent absorption band observed at 1127 $cm^{-1}$is attributed to the stretching vibration of the Ti-O bond. This band indicates the presence of titanium-oxygen linkages within the lattice structure and confirms the formation of titanium-based oxide units. The peak located at 957 cm^{-1} corresponds to the stretching vibration of the W-O bond. This band is typically associated with terminal W-O vibrations in tungsten oxide species and suggests the presence of coordinated tungsten in the oxide matrix. A distinct absorption band at 882 cm^{-1} is assigned to the stretching vibration of the terminal W=O bond. The presence of this band is characteristic of tungsten oxide structures and indicates the formation of oxo-functional groups (W=O), which play an important role in the structural and catalytic properties of tungsten-containing materials. The band appearing at 763 cm^{-1} is attributed to the bridging vibration of W-O-W linkages. This confirms the formation of a polymeric tungsten oxide network, where tungsten atoms are interconnected through oxygen bridges, contributing to structural stability and framework formation. Furthermore, the bands observed at 570 cm^{-1}

and 590 cm^{-1} are assigned to mixed metal-oxygen vibrations corresponding to Ti-O-W linkages. The presence of these peaks is particularly significant, as they indicate strong interaction between titanium and tungsten species. This confirms the formation of a heterometallic Ti-W oxide network rather than the mere physical mixture of individual TiO_2 and WO_3 phases.

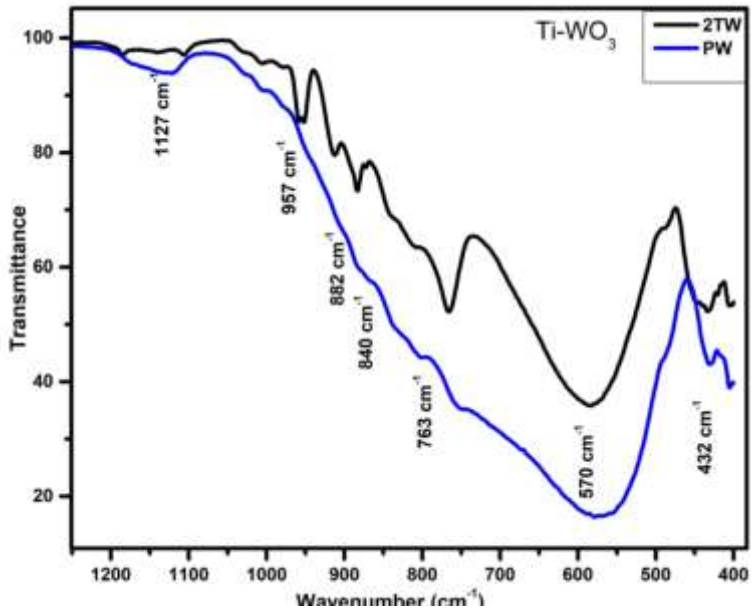


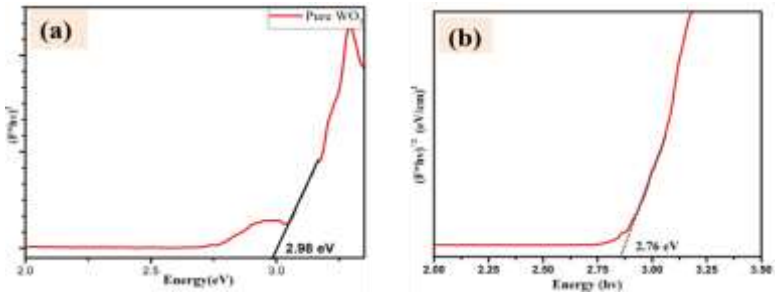
Figure.2 FTIR spectrums of series of doping Ti doped WO3 nanocomposite materials

Sr. No	Function group	Wavenumber (cm^{-1})	Force Constant ($dynes.cm^{-1}$)	Bond Length (Å)
1	Ti-O	1127	8.96×10^5	1.020
2	W-O	957	6.45×10^5	0.952
3	W=O	882	5.48×10^5	0.953
4	W-O-W	763	4.10×10^5	0.965
5	Ti-O W-O	570,590	2.29×10^5	0.954

UV-Diffuse Reflectance Spectrum (DRS) study:

The absorbance spectra of PW and BW are shown in Figure 3. The absorption is found for the PW is in the visible region range with a sharp absorption edge at around 416 nm. The PW sample exhibits an absorbance edge at 416 nm, corresponding to a calculated band gap energy of 2.98 eV. This relatively higher band gap indicates stronger electronic confinement and lower visible-light absorption capability. The value suggests that the material primarily absorbs in the near-UV region, which may limit its photocatalytic performance under visible light irradiation. In contrast, the 2TW sample shows a red shift in the absorbance edge to 449 nm, resulting in a reduced band gap energy of 2.76 eV. The observed decrease in band gap confirms the successful modification of the electronic

structure due to tungsten incorporation into the host lattice. The narrowing of the band gap enhances visible-light absorption, thereby improving the material's photocatalytic efficiency under solar irradiation. The shift of the absorption edge toward a longer wavelength (red shift) in the 2TW sample indicates the formation of intermediate energy levels within the band structure. This modification facilitates easier excitation of electrons from the valence band to the conduction band, thereby promoting effective charge carrier generation. Overall, the reduction in band gap energy from 2.98 eV (PW) to 2.76 eV (2TW) confirms that tungsten incorporation significantly improves the optical properties of the material, enhancing its suitability for visible-light-driven photocatalytic applications.



Samples	Absorbance edge (cm^{-1})	Band gap (eV)
PW	416	2.98
2TW	449	2.76

Activity Results:

Photocatalytic activity of Nanocomposite Materials:

The photocatalytic performance of Bi doped WO_3 was evaluated by investigating their catalytic efficiency under sun light irradiation. We used Methylene blue (cationic dye) with series of 2TW catalyst.

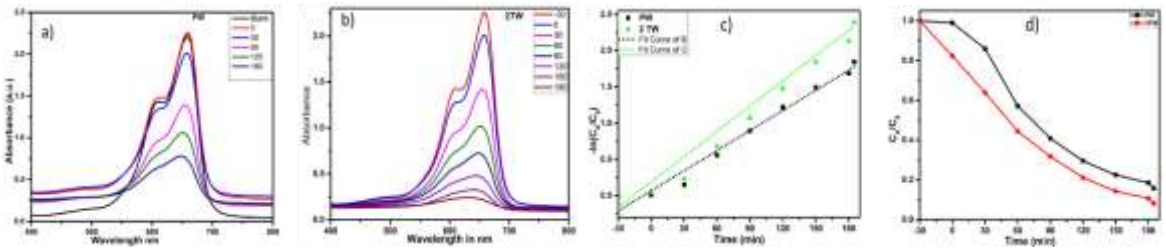


Figure 4: Comparative study of dye degradation a-b) testing of catalyst, c) kinetic study of catalyst, c) 2TW catalyst degradation graph with respect time.

The photocatalytic degradation of methylene blue (MB) over PW and 2TW samples was evaluated using UV-Visible absorption spectroscopy, and the results are presented in Fig. (a-d). Figure.4 (a) shows the time-dependent UV-Vis absorption spectra of MB in the presence of the PW sample under light irradiation. The characteristic absorption peak of MB

at approximately 664 nm gradually decreases with increasing irradiation time (0-180 min), indicating progressive degradation of the dye molecules. However, even after 180 min, a noticeable absorbance intensity remains, suggesting moderate photocatalytic activity of the PW sample. Figure (b) illustrates the corresponding spectral changes for the 2TW sample. A significantly faster reduction in the intensity of the MB absorption peak is observed compared to PW. The absorbance decreases sharply with irradiation time, and after 180 min, the peak intensity is drastically reduced, indicating superior degradation efficiency. The enhanced activity of 2TW may be attributed to improved charge separation and reduced electron–hole recombination due to tungsten incorporation. Figure (c) presents the kinetic analysis plotted as $-\ln(C/C_0)$ versus irradiation time. The linear relationship confirms that the degradation process follows pseudo-first-order kinetics. The slope of the linear fit represents the apparent rate constant (k). The 2TW sample exhibits a steeper slope than PW, indicating a higher reaction rate constant and faster degradation kinetics. Figure (d) shows the variation of normalized concentration (C/C_0) with irradiation time. The concentration of MB decreases steadily for both samples; however, the reduction is more pronounced in the case of 2TW. After 180 min of irradiation, 2TW achieves a significantly lower C/C_0 value compared to PW, confirming its higher photocatalytic efficiency.

Conclusion:

Overall, the results demonstrate that tungsten-modified 2TW exhibits enhanced photocatalytic performance for MB degradation compared to PW. The improved activity can be attributed to band gap narrowing, enhanced visible-light absorption, and efficient charge carrier separation, leading to increased generation of reactive species responsible for dye degradation. Investigation of Structural and optical property of Ti doped tungsten trioxide nano composites water remedial

Reference.

[1] C. Ray and T. Pal, “Recent advances of metal-metal oxide nanocomposites and their tailored nanostructures in numerous catalytic applications,” *J. Mater. Chem. A*, vol. 5, no. 20, pp. 9465–9487, 2017, doi: 10.1039/c7ta02116j.

[2] F. Zaera, “The new materials science of catalysis: Toward controlling selectivity by designing the structure of the active site,” *J. Phys. Chem. Lett.*, vol. 1, no. 3, pp. 621–627, 2010, doi: 10.1021/jz9002586.

[3] S. Rani, N. Bao, and S. C. Roy, “Solar spectrum photocatalytic conversion of CO 2 and water vapor into hydrocarbons using TiO 2 nanoparticle membranes,” *Appl. Surf. Sci.*, vol. 289, pp. 203–208, 2014, doi: 10.1016/j.apsusc.2013.10.135.

[4] K. Jain, A. S. Patel, V. P. Pardhi, and J. S. S. Flora, “Nanotechnology in Wastewater Management : A New Paradigm,” *Molecules*, vol. 26, p. 1797, 2021.

[5] Z. Abdin *et al.*, “Solar energy harvesting with the application of nanotechnology,” *Renew. Sustain.*

Energy Rev., vol. 26, pp. 837–852, 2013, doi: 10.1016/j.rser.2013.06.023.

[6] P. T. Sekoai *et al.*, "Application of nanoparticles in biofuels: An overview," *Fuel*, vol. 237, no. July 2018, pp. 380–397, 2019, doi: 10.1016/j.fuel.2018.10.030.

[7] A. D. Terna, E. E. Elemike, J. I. Mbonu, O. E. Osafile, and R. O. Ezeani, "The future of semiconductors nanoparticles: Synthesis, properties and applications," *Mater. Sci. Eng. B Solid-State Mater. Adv. Technol.*, vol. 272, no. December 2020, p. 115363, 2021, doi: 10.1016/j.mseb.2021.115363.

[8] Y. S. Pestovsky and A. Martínez-Antonio, "The use of nanoparticles and nanoformulations in agriculture," *J. Nanosci. Nanotechnol.*, vol. 17, no. 12, pp. 8699–8730, 2017, doi: 10.1166/jnn.2017.15041.

[9] H. Fukui, *Development of New Cosmetics Based on Nanoparticles*. Elsevier B.V., 2018. doi: 10.1016/B978-0-444-64110-6.00008-1.

[10] S. Sharma *et al.*, "Fueling a hot debate on the application of TiO2 nanoparticles in sunscreen," *Materials (Basel).*, vol. 12, no. 14, 2019, doi: 10.3390/ma12142317.

[11] W. Park and K. Na, "Advances in the synthesis and application of nanoparticles for drug delivery," *Wiley Interdiscip. Rev. Nanomedicine Nanobiotechnology*, vol. 7, no. 4, pp. 494–508, 2015, doi: 10.1002/wnan.1325.

[12] A. Tricoli, M. Righettoni, and A. Teleki, "Semico nductor gas sensors: Dry synthesis andapplication," *Angew. Chemie - Int. Ed.*, vol. 49, no. 42, pp. 7632–7659, 2010, doi: 10.1002/anie.200903801.

[13] H. Zheng, J. Z. Ou, M. S. Strano, R. B. Kaner, A. Mitchell, and K. Kalantar-Zadeh, "Nanostructured tungsten oxide - Properties, synthesis, and applications," *Adv. Funct. Mater.*, vol. 21, no. 12, pp. 2175–2196, 2011, doi: 10.1002/adfm.201002477.

[14] K. J. Lethy, D. Beena, V. P. Mahadevan Pillai, and V. Ganesan, "Bandgap renormalization in titania modified nanostructured tungsten oxide thin films prepared by pulsed laser deposition technique for solar cell applications," *J. Appl. Phys.*, vol. 104, no. 3, 2008, doi: 10.1063/1.2953070.

[15] F. Wang, C. DiValentin, and G. Pacchioni, "Rational Band Gap Engineering of WO 3 Photocatalyst for Visible light Water Splitting," *ChemCatChem*, vol. 4, no. 4, pp. 476–478, 2012, doi: 10.1002/cctc.201100446.

[16] H. Shinguu, M. M. H. Bhuiyan, T. Ikegami, and K. Ebihara, "Preparation of TiO2/WO3 multilayer thin film by PLD method and its catalytic response to visible light," *Thin Solid Films*, vol. 506–507, pp. 111–114, 2006, doi: 10.1016/j.tsf.2005.08.312.